



Smooth and stable.

Target Detachable Coils deliver consistently smooth deployment and exceptional microcatheter stability. Designed to work seamlessly together for framing, filling and finishing. Target Coils deliver the high performance you demand.

For more information, please visit www.strykerneurovascular.com/Target or contact your local Stryker Neurovascular sales representative.



Target™
DETACHABLE COILS

Computerised tomography and magnetic resonance imaging of laryngeal squamous cell carcinoma: A practical approach

Francesco Agnello¹, Francesco Cupido², Gianvincenzo Sparacia¹, Federico Midiri³, Martina Miroddi³, Emanuele Grassedonio¹ and Massimo Galia¹

Abstract

Squamous cell carcinoma is the most common head and neck cancer. This review describes the state-of-the-art computerised tomography and magnetic resonance imaging protocols of the neck and the normal larynx anatomy, and provides a practical approach for the diagnosis and staging of laryngeal squamous cell carcinoma.

Keywords

Computerised tomography, magnetic resonance imaging, squamous cell carcinoma

Introduction

Laryngeal cancer is one of most common head and neck cancer.¹ Squamous cell carcinoma (SCC) accounts for the majority of cases.² Other, less common, tumours include chondrosarcoma, metastases and non-Hodgkin's lymphoma.²

SCC is most common in the fifth to seventh decades of life.³ The male-to-female ratio is 3.83:1.³ Moderate or heavy alcohol consumption and smoking are the main risk factors for SCC.⁴ Workplace exposure to wood dust and paint fumes also increases the risk for SCC.⁴ An association between laryngeal tumour and human papilloma virus infection has also been reported.⁵

Unlike most non-squamous cell tumours, which are submucosa-based lesions, SCCs arise from the mucosa and, therefore, can be easily visualised at laryngoscopy, and biopsied.^{6,7}

The principal role of radiologic examinations is to evaluate deep tumour extent and anatomic relationship with surrounding structures, which can be missed at endoscopy and physical examination. Moreover, radiologic examinations allow simultaneous evaluation of neck lymph nodes and distant metastases.

In this paper, we will describe the state-of-the-art computerised tomography (CT) and magnetic resonance imaging (MRI) protocols, the normal larynx anatomy, and we offer a practical approach for diagnosis and staging of laryngeal SCC.

Imaging techniques

Radiologic evaluation of the larynx usually starts with CT because of short scanning time, excellent anatomic resolution, and wide availability. MRI is reserved for select cases, when CT results are not conclusive. Due to its excellent soft-tissue resolution, MRI is more accurate than CT in delineating deep tumour extension and cartilage involvement.

Image quality strongly depends on patient cooperation. At our hospital, patients are instructed not to swallow or cough during the acquisition in order to prevent or minimise motion-related artifacts before scanning.

CT. CT of the neck extends from the skull base to the inferior aortic arch. Patients are placed in the supine position, with the neck slightly extended.⁸ Intravenous contrast material is routinely used because it improves the delineation of the tumour extent and detection of neck lymph nodes. A delay of 50–75 s allows an

¹Department of Radiology, University of Palermo, Italy

²Department of Surgical and Oncological Sciences, University of Palermo, Italy

³School of Medicine, University of Palermo, Italy

Corresponding author:

Gianvincenzo Sparacia, Department of Radiology, University of Palermo, Italy Via del Vespro, 127 90127 – Palermo, Italy.

Email: gianvincenzo.sparacia@unipa.it

adequate enhancement of primary tumour and an accurate differentiation of cervical lymph nodes from vessels.⁹ Demonstration of sufficient attenuation of neck vessels suggests good image quality.¹⁰ Unenhanced images are not routinely acquired to reduce patient exposure to ionising radiations. At our hospital, unenhanced images are acquired only during the first CT examination.

A correct reformation plane orientation is crucial for avoiding misinterpretation. Axial images must be parallel to the true vocal cords or the hyoid bone, while coronal images must be parallel to the airways and orthogonal to the true vocal cords. Recognition of the true vocal cords is facilitated by the identification of the arythenoid cartilages.

Images are viewed using both soft-tissue (window width, 250–350 HU; window centre, 50 HU) and bone window-settings (window width, 2000 HU; window centre, 600 HU), the latter helps to evaluate cartilage invasion. Slice thickness is 2 mm with an overlapping reconstruction interval of 1 mm.

Multiplanar-reformatted (MPR) images in coronal and sagittal planes allow a more confident evaluation of the anatomic relationship between the tumour and the surrounding structures.

MRI. Magnetic resonance (MR) images are acquired using an anterior surface head and neck coil. Scan extent and patient position are similar to CT. The basic MRI protocol consists of axial and sagittal unenhanced T1 turbo spin echo (TSE) weighted sequences, axial fat-suppressed T2-weighted TSE sequence, axial diffusion-weighted sequence, and axial and coronal fat-suppressed T1-weighted TSE sequences obtained before and after gadolinium injection. Slice thickness is 2–4 mm, with no interslice gap. Similarly to CT, axial images must be parallel to the true vocal cords. To obtain the correct orientation, MR examination should start with the acquisition of an unenhanced sagittal T1-weighted sequence, which helps identify the larynx and the plane of the true vocal cords. Since fat shows bright signal intensity, unenhanced T1-weighted images also help delineate tumoral invasion of fat planes.

T2-weighted sequences are used to detect intratumoral cystic areas and evaluate deeper tumour spread.

DWI sequences are useful in detecting and characterising laryngeal mass, and in differentiating malignant from benign cervical lymph nodes.¹¹ Moreover, DWI seems to be promising in differentiating benign post-treatment changes and residual or recurrent tumour.^{12,13}

Intravenous contrast material administration is strongly recommended because it increases tumour conspicuity, helps differentiate necrotic and cystic areas from viable tumour, and improves the evaluation of soft tissue and perineural invasion.¹⁴ Fat saturation is essential in differentiating enhancing tumour from surrounding fat.

The use of a 3D fat-suppressed T1-weighted gradient echo (GRE) sequence (VIBE (Siemens Healthcare), LAVA (GE Healthcare) and THRIVE (Philips Healthcare)) taking approximately 30 s reduces the long acquisition times of traditional spin echo (SE) or fast SE sequences (several minutes) without degrading image quality, and motion artifacts.¹⁵

Anatomy of the larynx

Familiarity with the anatomy of the larynx, and the routes of spread of SCC is crucial in assigning the correct stage.

The larynx is anatomically divided into three parts: the supraglottis, glottis and subglottis (Figure 1).

The glottis and supraglottis are the most common sites of origin of SCC, and account for approximately 60% and 35% of cases, respectively. The remaining origins are in the subglottis or involve more than one area.¹ In the latter case, the tumour is classified as transglottic.

The supraglottis is the upper part of the larynx, and extends from the tip of the epiglottis to the laryngeal ventricles. Above the tip of the epiglottis is the oropharynx. The supraglottis includes the epiglottis, aryepiglottic folds, false vocal cords, and laryngeal ventricles. The glottis is located between the supraglottis and subglottis. It is bordered superiorly by the upper margin of the true vocal cords, and inferiorly by a plane 1 cm below the ventricles. The supraglottis contains the true vocal cord, and anterior and posterior commissures. The arytenoids cartilages are an useful anatomic landmark to differentiate the glottis from the supraglottis. Indeed, the superior board lies at the level of the false vocal cords, while the vocal process lies at the level of the true vocal cords.

The subglottis is the lower part of the larynx, and is separated by the trachea from the lower margin of the cricoid cartilage, which is easy to identify because it is the only laryngeal cartilage that forms a complete ring.

Diagnosis of SCC

The normal larynx wall is usually thin and symmetric. Any asymmetric thickening of the laryngeal wall should raise the suspicion of SCC (Figure 2 and 3).

At CT, SCCs usually show slight to moderate enhancement, which helps delineate tumour margins and evaluate deep tumour extension.⁹

At MR, SCCs show a characteristic T2-hyperintensity and T1-hypointensity. The former helps differentiate the tumour from hypointense muscle, while the latter helps differentiate the tumour from hyperintense fat.¹⁴ Hyperintensity on high-b-value diffusion-weighted images, and hypointensity on the apparent diffusion coefficient (ADC) map help detect the tumour, and confirm its solid nature.¹⁶

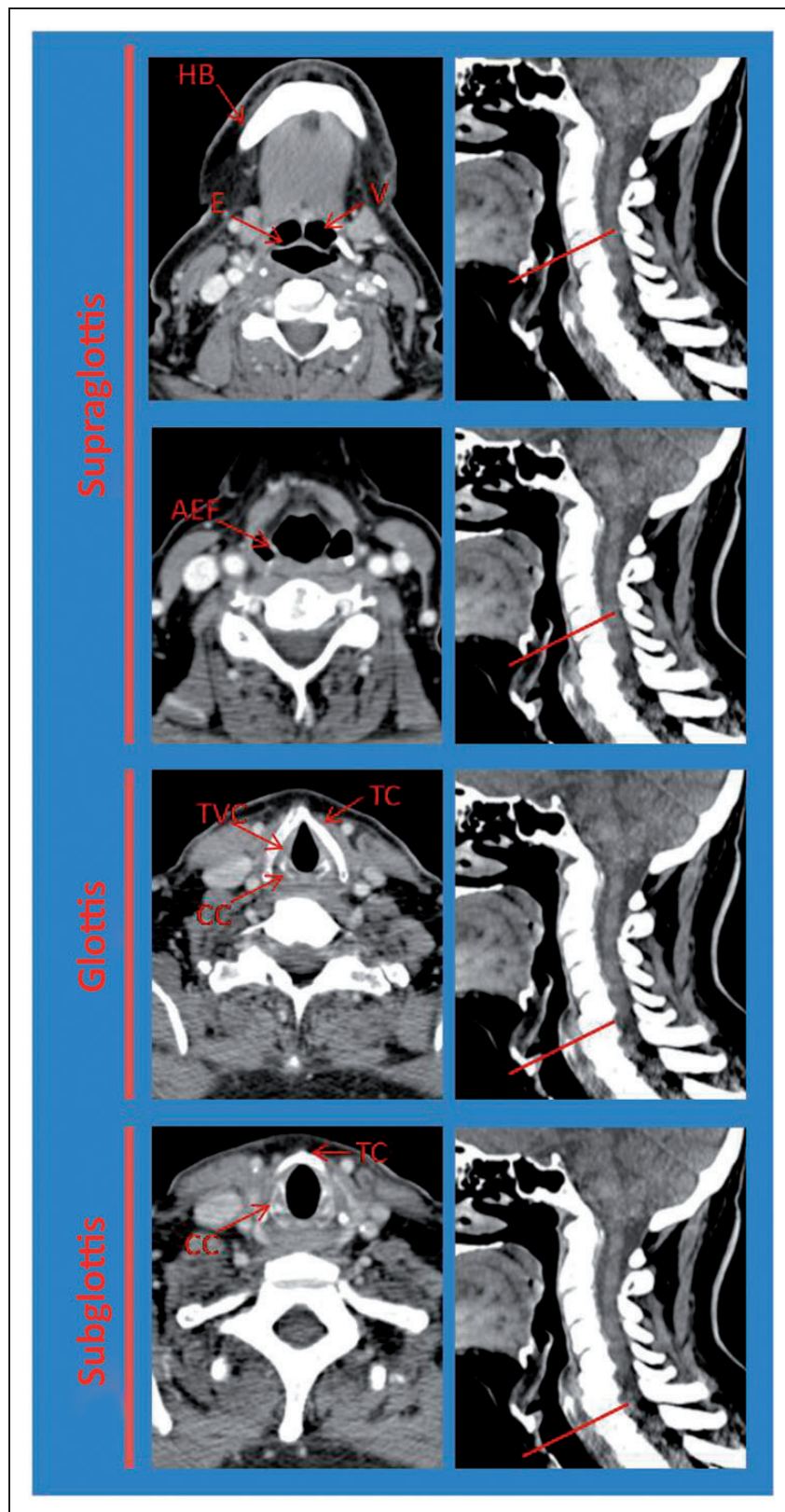


Figure 1. Anatomy of the larynx. AEF: aryepiglottic fold; CC: cricoid cartilage; E: epiglottis; HB: hyoid bone; LV: laryngeal ventricle; TVC: true vocal cords; TC: thyroid cartilage; V: vallecula.

SCC staging

SCC of the larynx is staged using the TNM criteria, which are endorsed by the American Joint Committee on Cancer Staging.¹⁷ The T stage is

based on tumour size and local extent, while the presence and location of regional nodal metastases define the N stage. The M stage indicates the presence or absence of haematogenous metastases.



Figure 2. Axial contrast-enhanced computerised tomography (CT) image obtained in a 56-year-old man with glottic squamous cell carcinoma (SCC) shows asymmetric thickening of the left true vocal cordal (arrowhead).

Local tumour spread. In addition to diagnosing an SCC, the radiologist should define its relationship to submucosal spaces, laryngeal cartilages and extra-laryngeal soft-tissues, because their involvement can preclude conservative surgery and radiation therapy.

The submucosal pre-epiglottic and paraglottic spaces are critical structures for the spread of SCC. Invasion of these spaces upstages SCC to T3 stage, thus influencing treatment choice.

The pre-epiglottic space is a triangular, fat-filled area located between the epiglottis (posteriorly) and the hyoid bone (anteriorly). The paraglottic spaces are located lateral to the true and false vocal cords, and contain fat and muscle. Of note, pre-epiglottic and paraglottic spaces cannot be visualised at laryngoscopy.

The primary sign of submucosal invasion at CT and MRI is an enhancing tumour within the submucosal spaces (Figure 4). Demonstration of replacement of T1-hypointense fat from hypo-intense tumour usually corroborates the diagnosis.

The presence of cartilage invasion indicates a T4 stage.¹⁷ The imaging appearance of the laryngeal cartilages depends on the degree of mineralisation. At CT, cortical ossified cartilage shows bone attenuation, while medullary fat and non-ossified cartilage show low attenuation. Tumour invasion can be suspected only in the presence of tumour proximity to the cartilage and asymmetric sclerosis of the cartilage surface¹⁸ (Figure 5).

MRI shows higher sensitivity than CT in the detection of cartilage tumour invasion.¹⁸ Normal cartilages

show variable signal intensity on T1- and T2-weighted images, depending on the degree of cartilage mineralisation, and no enhancement.^{18,19} Invaded cartilage show intermediate T2-signal intensity and variable enhancement.^{18,19}

A similar cartilage MRI appearance, however, can be due to peri-tumoral inflammation and reduces MRI specificity.^{18,19} Comparison with signal intensity of the primary tumour helps in the differential diagnosis: invaded cartilage shows T2-signal intensity and enhancement similar to that of the primary tumour, while inflamed cartilage shows T2-signal intensity and enhancement higher than that of the primary tumour.¹⁹

Lymphatic spread. Cervical lymph node metastasis is the main mechanism of the spread of SCC. Cervical nodes are located according to the classification of the American Head and Neck Society and the American Academy of Otolaryngology-Head and Neck Surgery.²⁰ This classification divides cervical nodes into six levels on the basis of the primary lymphatic drainage of each cervical tumour. Knowledge of nodal drainage patterns helps radiologists to correctly characterise enlarged nodes, and to accurately evaluate the most likely sites of metastasis.²¹ Indeed, the supra-glottis drains primarily into the upper jugular lymph nodes, while the glottis and subglottis have a sparse lymphatic drainage.²¹ These differences are due to the different embryologic origins of the supra-glottis with respect to those of the glottis and subglottis.²¹

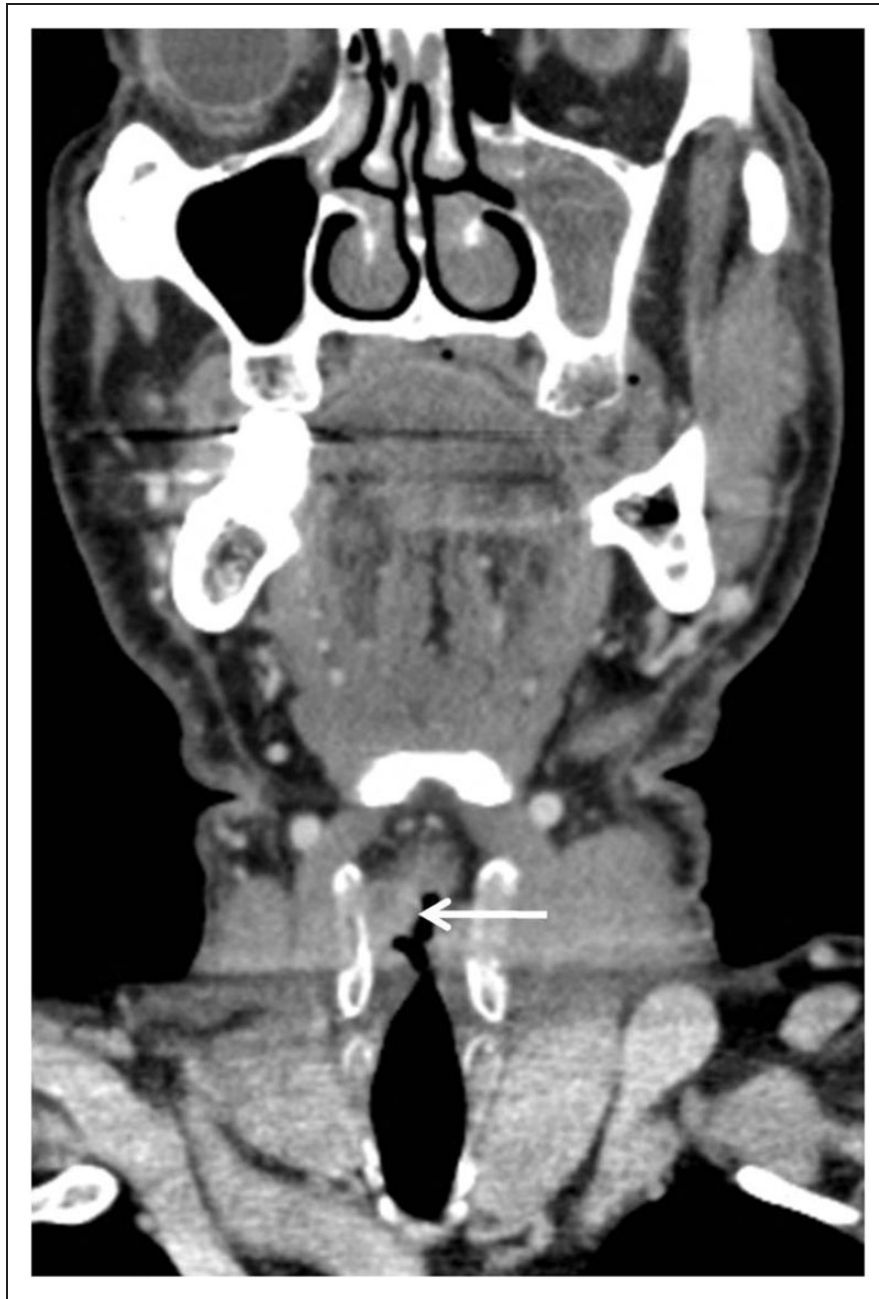


Figure 3. Coronal contrast-enhanced computerised tomography (CT) image obtained in a 65-year-old man shows a trans-glottic squamous cell carcinoma (SCC) (arrow) involving the true and false right vocal cord.

CT and MRI show higher accuracy than clinical examination in the detection of cervical lymph node metastasis.

The presence, number, site, and size of lymph node metastasis reflect tumour aggressiveness, and influence treatment choices.

Traditional criteria to differentiate normal and pathologic nodes include size, shape, margins and enhancement. Diffusion-weighted imaging is a promising technique to detect metastatic cervical node.

An enlarged cervical node should always raise the suspicion of metastasis (Figure 6). As a general rule, the smaller the size, the higher the likelihood of benignity. Several size cut-offs to differentiate normal from

pathologic cervical nodes have been reported in the literature, and range between 5–30 mm.²¹ For instance, the Response Evaluation Criteria in Solid Tumors (RECIST) version 1.1 criteria use the node short-axis diameter on axial CT and MR images. Nodes with short-axis diameter of <10 mm are considered benign, while those with a short-axis diameter of >15 mm are considered malignant.²² An optimal size cut-off, however, does not exist. Indeed, reactive lymph nodes can be enlarged due to hyperplasia and inflammation, and small lymph nodes can be pathologic due to microscopic metastatic deposits.²³ At our hospital, a cut-off short-axis diameter of 10 mm is used as suggested by Van den Brekel et al.²³

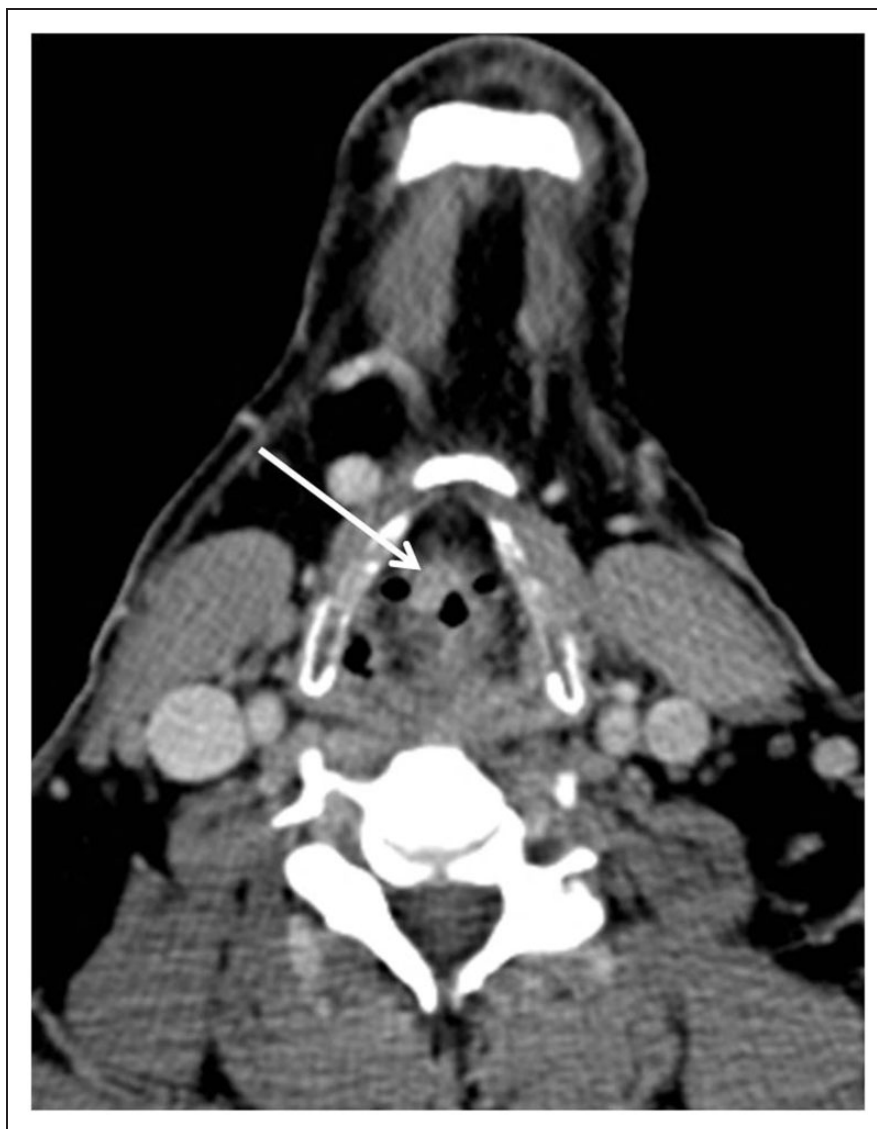


Figure 4. Axial contrast-enhanced computerised tomography (CT) image obtained in a 55-year-old man with supra-glottic squamous cell carcinoma (SCC) shows tumour invasion of the pre-epiglottic space (arrow).

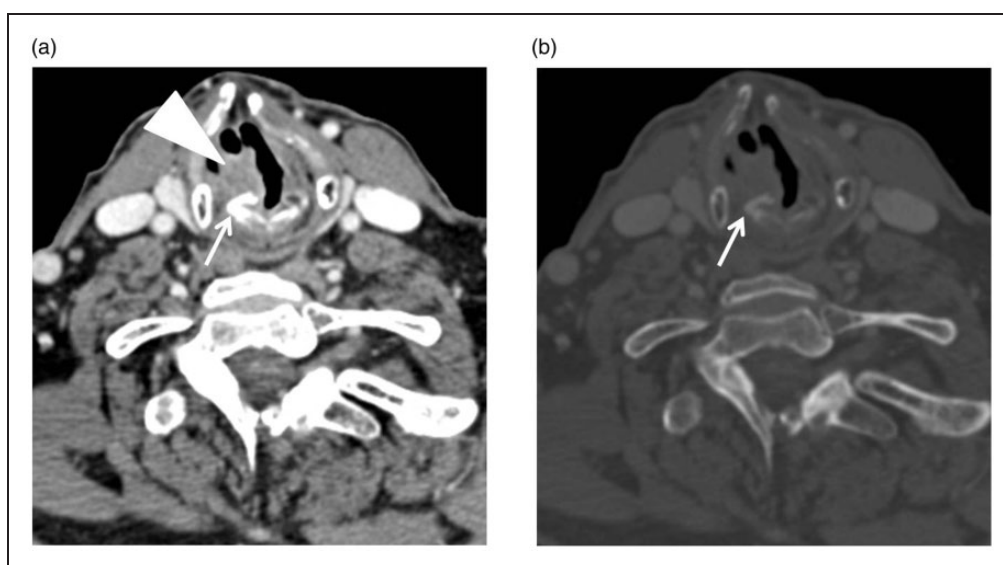


Figure 5. Axial contrast-enhanced computerised tomography (CT) images ((a) soft-tissue window, (b) bone window) obtained in a 76-year-old man with squamous cell carcinoma (SCC) of the right true vocal cord shows asymmetric sclerosis of the vocal process of the arytenoid cartilage (arrow) due to invasion of the tumour (arrowhead).

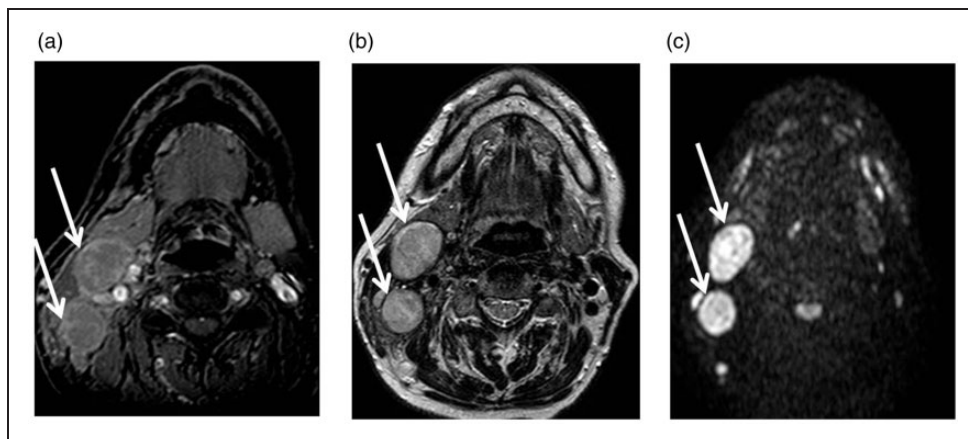


Figure 6. Axial magnetic resonance images obtained in a 66-year-old man with subglottic squamous cell carcinoma (SCC) and enlarged lymph node metastases in the level IIa and b on the right side. (a) On T2-weighted turbo spin echo (TSE) image, lymph node metastases (arrows) show heterogeneous hyperintensity. (b) On b800 diffusion-weighted image lymph node metastases show strong hyperintensity. (c) On contrast-enhanced T1-gradient echo (GRE) image lymph node metastases show heterogeneous enhancement.

Benign lymph nodes are typically oval- or flat-shaped, while malignant lymph nodes tend to be round. A longitudinal-to-axial largest diameter ratio equal to or greater than two suggests a benign lymph node.²⁴

Benign lymph nodes show well-defined margins.²¹ Ill-defined margins are a hallmark of malignancy and indicate extra-capsular tumour spread.²¹

Benign lymph nodes show a characteristic homogeneous enhancement, except for the hypoattenuating/intense fatty hilum, while metastatic nodes show a heterogeneous enhancement due to necrosis, haemorrhage or cystic degeneration.²¹

Several studies have demonstrated that metastatic lymph nodes have a lower ADC values than benign lymph nodes due to their increased cellularity.^{25–27} De Bondt et al. have reported that the use of ADC values in combination with the traditional imaging criteria improves the differentiation of malignant and benign lymph nodes.²⁵ It should be kept in mind, however, that reactive lymph nodes can sometimes show low ADC values due to a large amount of inflammatory cells and a fibrotic stroma.²⁸ In addition to diagnosing a lymph node metastasis, the radiologist should evaluate its relationship with surrounding structures such as carotid artery, muscle and bone since their involvement can preclude surgery. Carotid artery invasion should be suspected in presence of loss of fat plane; wall irregularity, vessel deformation and $>180\text{--}270^\circ$ circumferential encasement.²⁹

Haematogeneous spread. Haematogeneous metastases are uncommon, and are usually due to recurrent disease.^{30,31} Risk factors include clinically palpable neck lymph nodes, histological evidence of nodal metastasis and extracapsular spread.^{30–32} The lung is the most common site, representing 66% of haematogeneous metastases.³¹ Differential diagnosis between lung metastasis from SCC and synchronous primary SCC



Figure 7. Axial contrast-enhanced computerised tomography (CT) image obtained in a 68-year-old-man with glottic squamous cell carcinoma (SCC) and synchronous SCC of the lung shows a large mass in the superior lobe of the right lung. Diagnosis of primary SCC of the lung was done after biopsy and collegial revision.

is not easy (Figure 7). Other sites include the bone, liver, skin, mediastinum and bone marrow.³¹ Pre- and post-operative CT screening for distant metastases for distant metastases should be performed only in high-risk patients.

Funding

This research received no specific grant from any funding agency in the public, commercial, or not-for-profit sectors.

Conflict of interest

The authors declared no potential conflicts of interest with respect to the research, authorship, and/or publication of this article.

References

1. American Cancer Society. Laryngeal and hypopharyngeal cancer, <http://www.cancer.org/cancer/laryngealand-hypopharyngealcancer/detailedguide/laryngeal-and-hypopharyngeal-cancer-key-statistics> (2016, accessed 2 October 2016).
2. Greenlee RT, Hill-Harmon MB, Murray T, et al. Cancer statistics, 2001. *CA Cancer J Clin* 2001; 51: 15-36. Erratum in: *CA Cancer J Clin* 2001; 51: 144.
3. Marchiano E, Patel DM, Patel TD, et al. Subglottic squamous cell carcinoma: A population-based study of 889 cases. *Otolaryngol Head Neck Surg* 2016; 154: 315-321.
4. Blot WJ, McLaughlin JK, Winn DM, et al. Smoking and drinking in relation to oral and pharyngeal cancer. *Cancer Res* 1988; 48: 3282-3287.
5. Torrente MC, Rodrigo JP, Haigentz M, Jr, et al. Human papillomavirus infections in laryngeal cancer. *Head Neck* 2011; 33: 581-586.
6. De Foer B, Hermans R, Van der Goten A, et al. Imaging features in 35 cases of submucosal laryngeal mass lesions. *Eur Radiol* 1996; 6: 913-919.
7. Saleh EM, Mancuso AA and Stringer SP. CT of submucosal and occult laryngeal masses. *J Comput Assist Tomogr* 1992; 16: 87-93.
8. The American College of Radiology. ACR-ASNR-SPR practice parameter for the performance of computed tomography (ct) of the extracranial head and neck. <http://www.acr.org/~media/3e9cfc1876e84169a1adfbac2f2f06a3.pdf> (accessed 1 October 2016).
9. Keberle M, Tschammler A, Berning K, et al. Spiral CT of the neck: When do neck malignancies delineate best during contrast enhancement? *Eur Radiol* 2001; 11: 1986-1990.
10. Groell R, Doerfler O, Schaffler GJ, et al. Contrast-enhanced helical CT of the head and neck: Improved conspicuity of squamous cell carcinoma on delayed scans. *AJR Am J Roentgenol* 2001; 176: 1571-1575.
11. King AD, Ahuja AT, Yeung DK, et al. Malignant cervical lymphadenopathy: Diagnostic accuracy of diffusion-weighted MR imaging. *Radiology* 2007; 245: 806-813.
12. Zbären P, Caversaccio M, Thoeny HC, et al. Radionecrosis or tumor recurrence after radiation of laryngeal and hypopharyngeal carcinomas. *Otolaryngol Head Neck Surg* 2006; 135: 838-843.
13. Abdel Razek AA, Kandeel AY, Soliman N, et al. Role of diffusion-weighted echo-planar MR imaging in differentiation of residual or recurrent head and neck tumors and posttreatment changes. *AJNR Am J Neuroradiol* 2007; 28: 1146-1152.
14. Keberle M, Kenn W and Hahn D. Current concepts in imaging of laryngeal and hypopharyngeal cancer. *Eur Radiol* 2002; 12: 1672-1683.
15. Kataoka M, Ueda H, Koyama T, et al. Contrast-enhanced volumetric interpolated breath-hold examination compared with spin-echo T1-weighted imaging of head and neck tumors. *AJR Am J Roentgenol* 2005; 184: 313-319.
16. Thoeny HC, De Keyzer F and King AD. Diffusion-weighted MR imaging in the head and neck. *Radiology* 2012; 263: 19-32.
17. Edge SB, Byrd DR, Compton CC, et al. (eds) *AJCC cancer staging manual*. 7th ed. 2010. New York: Springer, 2010.
18. Becker M, Zbären P, Laeng H, et al. Neoplastic invasion of the laryngeal cartilage: Comparison of MR imaging and CT with histopathologic correlation. *Radiology* 1995; 194: 661-669.
19. Becker M, Zbären P, Casselman JW, et al. Neoplastic invasion of laryngeal cartilage: Reassessment of criteria for diagnosis at MR imaging. *Radiology* 2008; 249: 551-559.
20. Robbins KT, Clayman G, Levine PA, et al. American Head and Neck Society; American Academy of Otolaryngology-Head and Neck Surgery. Neck dissection classification update: Revisions proposed by the American Head and Neck Society and the American Academy of Otolaryngology-Head and Neck Surgery. *Arch Otolaryngol Head Neck Surg* 2002; 128: 751-758.
21. Hoang JK, Vanka J, Ludwig BJ, et al. Evaluation of cervical lymph nodes in head and neck cancer with CT and MRI: Tips, traps, and a systematic approach. *AJR Am J Roentgenol* 2013; 200: W17-W25.
22. Schwartz LH, Bogaerts J, Ford R, et al. Evaluation of lymph nodes with RECIST 1.1. *Eur J Cancer* 2009; 45: 261-267.
23. Van den Brekel MW, Stel HV, Castelijns JA, et al. Cervical lymph node metastasis: Assessment of radiologic criteria. *Radiology* 1990; 177: 379-384.
24. Steinkamp HJ, Cornehl M, Hosten N, et al. Cervical lymphadenopathy: Ratio of long- to short-axis diameter as a predictor of malignancy. *Br J Radiol* 1995; 68: 266-270.
25. De Bondt RB, Hoerberigs MC, Nelemans PJ, et al. Diagnostic accuracy and additional value of diffusion-weighted imaging for discrimination of malignant cervical lymph nodes in head and neck squamous cell carcinoma. *Neuroradiology* 2009; 51: 183-192.
26. Holzapfel K, Duetsch S, Fauser C, et al. Value of diffusion-weighted MR imaging in the differentiation between benign and malignant cervical lymph nodes. *Eur J Radiol* 2009; 72: 381-387.
27. Vandecasteele V, De Keyzer F, Vander Poorten V, et al. Head and neck squamous cell carcinoma: Value of diffusion-weighted MR imaging for nodal staging. *Radiology* 2009; 251: 134-146.
28. Wang J, Takashima S, Takayama F, Kawakami S, et al. Head and neck lesions: Characterization with diffusion-weighted echo-planar MR imaging. *Radiology* 2001; 220: 621-630.
29. Yousem DM, Hatabu H, Hurst RW, et al. Carotid artery invasion by head and neck masses: Prediction with MR imaging. *Radiology* 1995; 195: 715-720.
30. Alvi A and Johnson JT. Development of distant metastasis after treatment of advanced-stage head and neck cancer. *Head Neck* 1997; 19: 500-505.
31. Ferlito A, Saha AR, Silver CE, et al. Incidence and sites of distant metastases from head and neck cancer. *ORL J Otorhinolaryngol Relat Spec* 2001; 63: 202-207.
32. Ljumanovic R, Langendijk JA, Hoekstra OS, et al. Distant metastases in head and neck carcinoma: Identification of prognostic groups with MR imaging. *Eur J Radiol* 2006; 60: 58-66.